ZZ boundary states and fragmented AdS_2 spaces

JHEP07(2009)002

(http://iopscience.iop.org/1126-6708/2009/07/002)

Published by IOP Publishing for SISSA

Received: *February 27, 2009*
Revised: *June 4, 2009*
Accepted: *June 11, 2009*
Published: *July 1, 2009*

JHEP07(2009)002

ZZ boundary states and fragmented AdS_2 spaces

Simone Giombi and Xi Yin

Center for the Fundamental Laws of Nature,
Jefferson Physical Laboratory, Harvard University,
Cambridge, MA 02138 U.S.A.

E-mail: giombi@physics.harvard.edu, xiyin@fas.harvard.edu

Abstract: In this paper we show that Liouville gravity on the strip with Zamolodchikov-Zamolodchikov (ZZ) boundary conditions has a semi-classical interpretation in terms of fragmented AdS_2 spacetime geometries. Further, we study the three-point functions of the ZZ boundary primaries, and show that they are dominated by multi-AdS_2 instantons in the classical limit.

Keywords: Field Theories in Lower Dimensions, 2D Gravity, Conformal and W Symmetry

ArXiv ePrint: 0808.0923

doi:10.1088/1126-6708/2009/07/002

Contents

1 Introduction

Two-dimensional gravity has been extensively explored in the past 30 years, both as the worldsheet description of string theories and as a toy model for higher dimensional quantum gravity (for a review see [1] and references therein). Quantum gravity in AdS_2, which is expected to be related to extremal black holes, remains mysterious [2–7]. In this paper, we shall take the viewpoint that "pure" quantum gravity in AdS_2 is described by Liouville gravity, with Zamolodchikov-Zamolodchikov (ZZ) boundary conditions [8].[1] The states of quantum gravity in global AdS_2 will be the boundary primaries of ZZ. This proposal will be validated by finding the semi-classical interpretation of these states and their correlation functions. We will see that in the semi-classical limit, the ZZ boundary primaries describe "fragmented" AdS_2's, i.e. several global AdS_2's "attached" along their boundaries. The correlation functions of the ZZ boundary primaries will be dominated by the contribution from classical instantons, which are several Poincaré discs suitably "glued" together along parts of their boundaries.

We analyze the quantum corrections to the two-fragmented AdS_2 using the exact bulk-boundary three point functions on the disc. The radius of the AdS_2 solution is large in the semi-classical (weak coupling) limit of Liouville gravity. In this limit, the Liouville theory has either large positive central charge c_L (with real background charge Q), or large negative

[1] For reviews of Liouville theory see for example [10, 11].

JHEP07(2009)002

c_L (with imaginary Q). In the $c_L > 0$ case, we find that quantum corrections erase one of the two AdS_2's. In the $c_L < 0$ case, the two-fragmented AdS_2 survive in the quantum theory.

From the point of view of AdS_2/CFT_1 correspondence, our results suggest that the "CFT_1" dual to pure Liouville gravity in AdS_2 comprises a single copy of Virasoro alegbra and a finite set of primary states – those of Liouville theory on a strip with ZZ boundary conditions. The correlation functions of these primaries can in principle be computed exactly using bootstrap methods, which then completely characterizes the theory.

The paper is organized as follows. In section 2 we first review the ZZ boundary conditions and boundary primaries. We will then probe the "geometry" of the semi-classical limit of the ZZ boundary primary using a bulk primary operator, and show that the boundary primaries can be identified as fragmented AdS_2's. In section 3 we study the three-point functions of the boundary primaries. Once again using the bulk primary probe, we will find that in the semi-classical limit the bulk-boundary four-point function is dominated by an instanton solution interpolating fragmented AdS_2's.

2 ZZ boundary primaries as fragmented AdS_2

2.1 ZZ boundary conditions and boundary primaries in Liouville theory

We work in the convention of [8], and write the Liouville Lagrangian density (in a flat background metric) as

$$\mathcal{L} = \frac{1}{4\pi}(\partial_a \phi)^2 + \mu e^{2b\phi}. \tag{2.1}$$

The background charge is $Q = b + 1/b$, and the central charge of the Liouville CFT is given by $c = 1 + 6Q^2$. Depending on whether b is real or purely imaginary, the central charge c is greater or less than 1. If b is imaginary, we may retain a real Lagrangian density by Wick rotating $\phi \to i\tilde{\phi}$, and $\tilde{\phi}$ will have a wrong sign kinetic term. The Liouville field ϕ can be thought of as the conformal mode of gravity in two dimensions, with metric

$$ds^2 = e^{2b\phi}\delta_{ab} d\sigma^a d\sigma^b. \tag{2.2}$$

The Liouville action is generated when a two-dimensional "matter" conformal field theory of nonzero central charge $-c$ is coupled to gravity [12]. For the purpose of this paper, we can ignore the matter CFT, although we shall keep in mind that the full theory of quantum gravity should have total central charge zero.

The ZZ boundary condition is such that the expectation value of $e^{2b\phi}$ goes to $+\infty$ at the boundary. Such consistent quantum boundary conditions are labeled by a pair of positive integers (m, n). There is a symmetry which exchanges m with n while sending $b \to 1/b$. Global AdS_2 can be described as a classical solution of Liouville theory on a strip $\sigma \in (0, \pi)$, $\tau \in \mathbf{R}$, with $e^{2b\phi} \to +\infty$ on the two boundaries. In the quantum theory, we can choose independently (m, n) boundary condition on the left side of the strip, and (m', n') on the right side of the strip. The Hilbert space of states on the strip will be denoted by $\mathcal{H}_{(m,n;m',n')}$. It consists of boundary primary states $\psi_{k,l}$ and their Virasoro descendants. The boundary primary $\psi_{k,l}$ is characterized by its conformal dimension

$$\Delta_{k,l} = \frac{Q^2}{4} - \frac{(kb + l/b)^2}{4}, \tag{2.3}$$

JHEP07(2009)002

and is subject to the selection rule

$$k = |m-m'|+1,\ |m-m'|+3,\ \cdots, m+m'-1;$$
$$l = |n-n'|+1,\ |n-n'|+3,\ \cdots, n+n'-1. \tag{2.4}$$

The bulk one-point function $\langle V_\alpha(z,\bar{z})\rangle$ on the disc with boundary condition (m,n), as well as the bulk-boundary two-point function (for special boundary operators), have been solved in [8]. We will need more: the bulk-boundary three-point function, boundary three-point function, and the bulk-to-boundary four-point function. These will be solved in the next few subsections by conformal bootstrap method.

2.2 Fragmented AdS_2 as classical solutions

It is well known that the Liouville equation of motion on the strip (for simplicity we set henceforth $\mu = 1$ in the action (2.1))

$$(\partial_\sigma^2 - \partial_t^2)\phi = 4\pi b e^{2b\phi} \tag{2.5}$$

admits the basic static solution

$$\phi = -\frac{1}{2b}\ln(4\pi b^2 \sin^2\sigma)\,. \tag{2.6}$$

Of course, the corresponding physical metric $ds^2 = e^{2b\phi}(-dt^2 + d\sigma^2)$ is nothing but the AdS_2 space-time. This is the $\mathrm{SL}(2,\mathbb{R})$ invariant vacuum of Liouville theory first pointed out in [13, 14] (see also [2]).

It is easy to see that the AdS_2 solution is part of a more general family of static solutions

$$\phi = -\frac{1}{2b}\ln\left(4\pi b^2 \frac{\sin^2(l\sigma)}{l^2}\right) \tag{2.7}$$

parameterized by an integer $l \geq 1$. These solutions behave like AdS_2 at the $\sigma = 0, \pi$ boundaries, but the metric also blows up in the "interior" at $\sigma = \frac{p}{l}\pi\,, p = 1, \cdots, l-1$. In other words, the corresponding space-time looks like l disconnected copies of the AdS_2 solution. An example with $l = 2$ is plotted in figure 1. We will refer to these solutions as "fragmented AdS_2 spaces".

A first hint to the relation between fragmented AdS_2's and ZZ boundary primaries comes from looking at the classical Liouville stress tensor evaluated on the solutions (2.7). The T_{00} component of the stress tensor for a static solution reads

$$T_{00} = \frac{1}{4\pi}(\partial_\sigma\phi)^2 + e^{2b\phi} - \frac{1}{2\pi b}\partial_\sigma^2\phi\,, \tag{2.8}$$

where the last term comes from the "linear dilaton" coupling to the 2d scalar curvature. Evaluated on (2.7), this just gives the constant $T_{00} = -\frac{l^2}{4\pi b^2}$. Then one would obtain an energy relative to the AdS_2 vacuum

$$E = -\frac{l^2-1}{4b^2}\,. \tag{2.9}$$

Note that this result precisely matches the classical limit $b \to 0$ of the conformal dimension $\Delta_{k,l}$ of the ZZ boundary primaries, eq. (2.3) (k drops out of the classical limit, as long as it is much smaller than $\frac{1}{b^2}$).

JHEP07(2009)002

2.3 The classical limit of bulk-boundary three point functions

A given ZZ boundary primary $|\psi\rangle$ should correspond to a deformation of the Liouville profile (i.e. the space-time metric) in the bulk. Specifically, we would like to argue that the relevant bulk metrics in the classical limit $b \to 0$ correspond to the "fragmented" AdS_2 spaces (2.7). To test this idea, we shall study the expectation value $\langle\phi\rangle$ of the Liouville field on the strip, in a boundary primary state $|\psi\rangle$. This can be done by using as a "probe" the bulk primary operator $V_\alpha = e^{2\alpha\phi}$. More precisely, we need to compute the disc bulk-boundary three point function

$$\langle\psi(y_1)\psi(y_2)V_\alpha(z,\bar{z})\rangle = |z-\bar{z}|^{-2\Delta_\alpha}(y_1-y_2)^{-2h}\mathcal{F}(\eta) \tag{2.10}$$

where $\Delta_\alpha = \alpha(Q-\alpha)$ is the dimension of V_α, h is the dimension of ψ, and η is the $\mathrm{SL}(2,\mathbb{R})$ invariant cross ratio

$$\eta = \frac{(z-\bar{z})(y_1-y_2)}{(z-y_2)(y_1-\bar{z})} = 1 - e^{2i\sigma}\,, \tag{2.11}$$

where σ is the spatial coordinate on the strip (to obtain this relation, one can use $\mathrm{SL}(2,\mathbb{R})$ to set $y_1 = 0\,, y_2 = \infty$). The three point function (2.10) is interpreted as the expectation value $\langle\psi|V_\alpha(\sigma)|\psi\rangle$ in the ZZ boundary primary $|\psi\rangle$. When ψ is the identity operator, this is just the bulk one-point function computed by ZZ [8]

$$\langle V_\alpha(z,\bar{z})\rangle = \frac{\mathrm{U}(\alpha)}{|z-\bar{z}|^{2\Delta_\alpha}}\,. \tag{2.12}$$

Transforming back to strip coordinates $z = e^{i\sigma+\tau}$, one can see that in fact this is just the AdS_2 metric (2.6).

The correlation function (2.10) depends of course on the explicit choice of (m,n) boundary conditions. For now we keep the analysis general and do not specify the type of boundary conditions. Let us consider the simplest nontrivial example, $\psi = \psi_{1,2}$. According to (2.3), it has conformal dimension

$$h_{1,2} = -\frac{1}{2} - \frac{3}{4b^2}. \tag{2.13}$$

All ZZ boundary primaries are degenerate, i.e. their conformal families contains null states. In particular, the conformal family of $\psi_{1,2}$ has a null state at level two, namely $(L_{-1}^2 + b^{-2}L_{-2})|\psi_{1,2}\rangle = 0$. It follows that the bulk-boundary three point function satisfies the differential equation

$$\left\{\partial_{y_1}^2 + b^{-2}\left[\frac{h_{1,2}}{(y_2-y_1)^2} + \frac{\Delta_\alpha}{(z-y_1)^2} + \frac{\Delta_\alpha}{(\bar{z}-y_1)^2} - \frac{\partial_{y_2}}{y_2-y_1} - \frac{\partial_z}{z-y_1} - \frac{\partial_{\bar{z}}}{\bar{z}-y_1}\right]\right\}\langle\psi_{1,2}(y_1)\psi_{1,2}(y_2)V_\alpha(z)\rangle = 0\,. \tag{2.14}$$

In terms of $\mathcal{F}(\eta)$, the equation is

$$\eta(\eta-1)\mathcal{F}''(\eta) + \left[(2+b^{-2})\eta - 2(1+b^{-2})\right]\mathcal{F}'(\eta) + b^{-2}\Delta_\alpha\frac{\eta}{\eta-1}\mathcal{F}(\eta) = 0\,. \tag{2.15}$$

JHEP07(2009)002

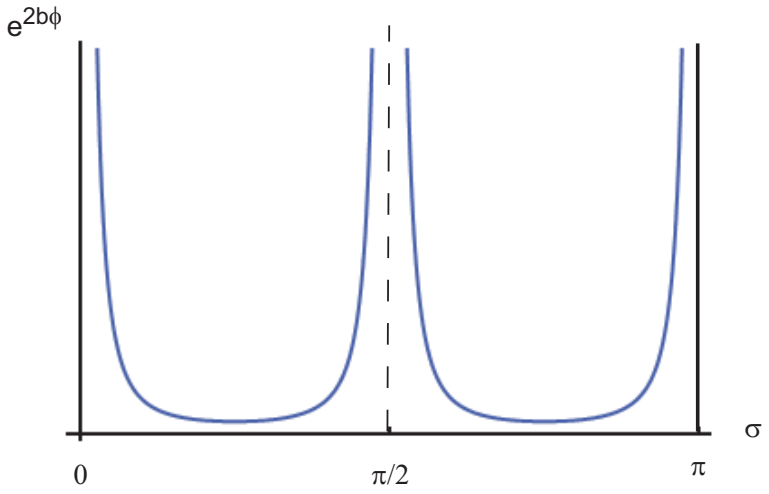

Figure 1. The "two-fragmented" AdS_2 space.

In the next subsection we will explicitly solve this equation at finite b and discuss in detail the results. Here we first present an easy way to arrive at the classical limit of the bulk-boundary three point function, hence the classical interpretation of the boundary primary $\psi_{k,l}$. The idea is that the equation (2.15) has a naive classical limit ($b \to 0$),

$$(\eta - 2)\mathcal{F}'_{cl}(\eta) + \Delta_\alpha \frac{\eta}{\eta - 1}\mathcal{F}_{cl}(\eta) = 0\,. \tag{2.16}$$

The solution is readily obtained

$$\mathcal{F}_{cl}(\eta = 1 - e^{2i\sigma}) = (\cos\sigma)^{-2\Delta_\alpha}\,, \tag{2.17}$$

where $\Delta_\alpha \simeq \alpha/b$. Combining with the prefactor $|z - \bar{z}|^{2\Delta_\alpha}$ and transforming to the strip, one obtains as expected the two-fragmented AdS_2 (see figure 1), i.e. $\langle\psi_{1,2}|V_\alpha(\sigma)|\psi_{1,2}\rangle \sim (\sin 2\sigma)^{-2\alpha/b}$. Note also that since the differential equation reduces to first order, the choice of boundary condition will not matter in this limit.

Let us now examine the bulk-boundary three point function involving $\psi_{1,3}$

$$\langle\psi_{1,3}(y_1)\psi_{1,3}(y_2)V_\alpha(z)\rangle = |z - \bar{z}|^{-2\Delta_\alpha}(y_1 - y_2)^{-2h_{1,3}}\mathcal{F}_{1,3}(\eta) \tag{2.18}$$

with $h_{1,3} = -1 - 2b^{-2}$. The conformal family of $\psi_{1,3}$ has a null state at level 3,

$$\left(L_{-1}^3 + 4b^{-2}L_{-2}L_{-1} + (2b^{-2} + 4b^{-4})L_{-3}\right)|\psi_{1,3}\rangle = 0 \tag{2.19}$$

The differential equation on the disc three point function is

$$\begin{aligned}\Big\{\partial_{y_1}^3 + 4b^{-2}\Big[&\frac{h_{1,3}}{(y_2 - y_1)^2} + \frac{\Delta_\alpha}{(z - y_1)^2} + \frac{\Delta_\alpha}{(\bar{z} - y_1)^2} - \frac{\partial_{y_2}}{y_2 - y_1} - \frac{\partial_z}{z - y_1} - \frac{\partial_{\bar{z}}}{\bar{z} - y_1}\Big]\partial_{y_1} \\ &+(2b^{-2} + 4b^{-4})\Big[\frac{2h_{1,3}}{(y_2 - y_1)^3} + \frac{2\Delta_\alpha}{(z - y_1)^3} + \frac{2\Delta_\alpha}{(\bar{z} - y_1)^3} - \frac{\partial_{y_2}}{(y_2 - y_1)^2} - \frac{\partial_z}{(z - y_1)^2} \\ &- \frac{\partial_{\bar{z}}}{(\bar{z} - y_1)^2}\Big]\Big\}\langle\psi_{1,3}(y_1)\psi_{1,3}(y_2)V_\alpha(z)\rangle = 0\,.\end{aligned} \tag{2.20}$$

In the $b \to 0$ limit (with Δ_α held fixed), the equation reduces to

$$(\eta-1)(\eta^2-3\eta+3)\mathcal{F}^{cl}_{1,3}{}'(\eta)+2\Delta_\alpha\eta(\eta-2)\mathcal{F}^{cl}_{1,3}(\eta)=0\,. \tag{2.21}$$

The solution is

$$\mathcal{F}^{cl}_{1,3}(\eta=1-e^{2i\sigma})=(1+2\cos(2\sigma))^{-2\Delta_\alpha}\,. \tag{2.22}$$

which precisely gives rise to the 3-fragmented AdS_2 after the z-dependent prefactor is included. In fact, we observe more generally that the conformal family of $\psi_{1,l}$ has a null state at level l, of the form (see page 245 of [16])

$$\det\left[-J_-+\sum_{m=0}^{l-1}b^{-2m}J_+^m L_{-m-1}\right]|\psi_{1,l}\rangle=0, \tag{2.23}$$

where the determinant is taken over an $l\times l$ matrix, with $J_\pm$ defined by

$$J_-=\begin{pmatrix}0&0&\cdots&0&0\\1&0&\cdots&0&0\\0&1&\cdots&0&0\\&&\cdots&&\\0&0&\cdots&1&0\end{pmatrix}_{l\times l},\qquad J_+=\begin{pmatrix}0&l-1&0&0&\cdots&0&0\\0&0&2(l-2)&0&\cdots&0&0\\0&0&0&3(l-3)&\cdots&0&0\\&&&&\cdots&&\\0&0&0&0&\cdots&0&l-1\\0&0&0&0&\cdots&0&0\end{pmatrix}_{l\times l}, \tag{2.24}$$

In particular, the classical limit of the null state equation for $\psi_{1,l}$ is given by $L_{-l}|\psi_{1,l}\rangle=\mathcal{O}(b^2)$. Writing

$$\langle\psi_{1,l}(y_1)\psi_{1,l}(y_2)V_\alpha(z)\rangle=|z-\bar{z}|^{-2\Delta_\alpha}(y_1-y_2)^{-2h_{1,l}}\mathcal{F}_{1,l}(\eta) \tag{2.25}$$

Analogously to (2.21), the classical constraining equation can be obtained as the first order differential equation

$$\eta(\eta-1)\mathcal{F}^{cl}_{1,l}{}'(\eta)+\Delta_\alpha\left[2-\eta+l\eta\frac{(1-\eta)^l+1}{(1-\eta)^l-1}\right]\mathcal{F}^{cl}_{1,l}(\eta)=0\,. \tag{2.26}$$

The solution is

$$\mathcal{F}^{cl}_{1,l}(\eta=1-e^{2i\sigma})=\left(\frac{\sin l\sigma}{\sin\sigma}\right)^{-2\Delta_\alpha} \tag{2.27}$$

Consequently,

$$\langle\psi_{1,l}|e^{2\alpha\phi(\sigma)}|\psi_{1,l}\rangle\sim(\sin l\sigma)^{-2\alpha/b}, \tag{2.28}$$

corresponding to the l-fragmented AdS_2, in accordance with our general proposal.

2.4 Quantum bulk-boundary three-point functions

2.4.1 General boundary condition

We shall now study the quantum bulk-boundary three point function (2.10) at finite coupling. We will specialize to the simplest non-trivial example $\psi=\psi_{1,2}$ (in section 2.5 we will propose a method to obtain the bulk-boundary three point function for general $\psi_{k,l}$). To

this purpose, we need to solve the second order differential equation (2.15) exactly at finite b. The equation can be put in the standard hypergeometric form, and the general solution is

$$\begin{aligned}\mathcal{F}(\eta) &= c_1(1-\eta)^{\alpha/b}{}_2F_1\left(\frac{2\alpha}{b}, 1+b^{-2}; 2+2b^{-2}; \eta\right)\\ &\quad + c_2(1-\eta)^{\alpha/b}\eta^{-1-2b^{-2}}{}_2F_1\left(-1-2b^{-2}+\frac{2\alpha}{b}, -b^{-2}; -2b^{-2}; \eta\right),\end{aligned} \tag{2.29}$$

where ${}_2F_1(A,B;C;z)$ is the Gauss hypergeometric function. The constants c_1 and c_2 are related to the factorization of the disc three point function along the boundary operator channels corresponding to the boundary primaries $\mathbf{1}$ (the identity operator) and $\psi_{1,3}$ (if it is allowed by the specific choice of boundary condition, according to the selection rules (2.4)). In particular,

$$\begin{aligned}c_1 &= \mathrm{U}(\alpha),\\ c_2 &= \langle\psi_{1,2}\psi_{1,2}\psi_{1,3}\rangle R_{1,3}(\alpha),\end{aligned} \tag{2.30}$$

where $\mathrm{U}(\alpha)$ is the coefficient of the disc one point function of V_α, and $R_{1,3}(\alpha)$ is the coefficient of the bulk-to-boundary two point function of V_α with $\psi_{1,3}$. By $\langle\psi_{1,2}\psi_{1,2}\psi_{1,3}\rangle$ we mean the coefficient of the corresponding boundary three point function, with the appropriate boundary conditions along the three segments of the boundary of the disc in between the operator insertions. Note that $\psi_{1,3}$ has conformal dimension $h_{1,3} = -1-2b^2$, $R_{1,3}(0) = 0$, and that both $R_{1,3}(\alpha)$ and $\langle\psi_{1,2}\psi_{1,2}\psi_{1,3}\rangle$ depend on the boundary conditions. The explicit expressions for $\mathrm{U}(\alpha)$ and $R_{1,3}(\alpha)R_{1,3}(-b/2)$ were derived by ZZ [8]. The boundary three point function $\langle\psi_{1,2}\psi_{1,2}\psi_{1,3}\rangle$, however, was not previously derived and will be obtained below.

Let us consider the classical/weak coupling limit of (2.29), i.e. small b. The asymptotics of the Gauss hypergeometric functions can be extracted using the quadratic transformation

$${}_2F_1(A,B;2B;z) = (1-z)^{-A/2}{}_2F_1\left(\frac{A}{2}, B-\frac{A}{2}; B+\frac{1}{2}; \frac{z^2}{4(z-1)}\right) \tag{2.31}$$

and the asymptotic expansion [15]

$${}_2F_1(A,B+\lambda;C+\lambda;z) = (1-z)^{-A}(1+\mathcal{O}(\lambda^{-1})), \qquad \lambda\to\infty. \tag{2.32}$$

We then find in the small b limit

$$\begin{aligned}\mathcal{F}(\eta) &\sim \mathrm{U}(\alpha)\left(1-\frac{\eta^2}{4(\eta-1)}\right)^{-\alpha/b} + \langle\psi_{1,2}\psi_{1,2}\psi_{1,3}\rangle R_{1,3}(\alpha)(1-\eta)^{\frac{1}{2}+b^{-2}}\eta^{-1-2b^{-2}}\left(1-\frac{\eta^2}{4(\eta-1)}\right)^{\alpha/b-\frac{1}{2}}\\ &= \mathrm{U}(\alpha)(\cos\sigma)^{-2\alpha/b} + \langle\psi_{1,2}\psi_{1,2}\psi_{1,3}\rangle R_{1,3}(\alpha)(-2i\sin\sigma)^{-1-2b^{-2}}(\cos\sigma)^{2\alpha/b-1}.\end{aligned} \tag{2.33}$$

In particular, in the $\alpha\to 0$ limit, $\mathcal{F}(\eta)\to 1$ as expected. After a conformal transformation back to the strip, we conclude that

$$\begin{aligned}\langle\psi_{1,2}|e^{2\alpha\phi(\sigma)}|\psi_{1,2}\rangle &\sim \mathrm{U}(\alpha)(\sin 2\sigma)^{-2\alpha/b}\\ &\quad + \langle\psi_{1,2}\psi_{1,2}\psi_{1,3}\rangle R_{1,3}(\alpha)(-i)^{-1-2b^{-2}}(2\sin\sigma)^{-1-2b^{-2}-2\alpha/b}(\cos\sigma)^{2\alpha/b-1}\end{aligned} \tag{2.34}$$

JHEP07(2009)002

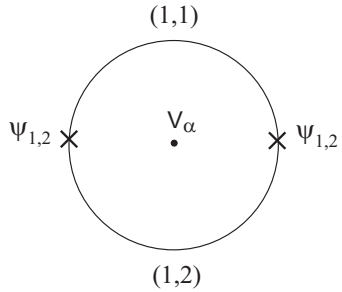

Figure 2. Depiction of the bulk-boundary three point function $\langle\psi_{1,2}(y_1)\psi_{1,2}(y_2)V_\alpha(z)\rangle$ with a specific choice of boundary condition.

as $b \to 0$ with α/b fixed. This can be compared to the vacuum expectation value of V_α, which as discussed in the previous section corresponds to the regular AdS_2 profile

$$\langle 1|e^{2\alpha\phi(\sigma)}|1\rangle \sim \mathrm{U}(\alpha)(2\sin\sigma)^{-2\alpha/b}\,. \tag{2.35}$$

If the second term in (2.34) is absent, i.e. ignoring the contribution from the $\psi_{1,3}$ channel, then the contribution from the identity operator channel suggests indeed that the boundary primary $\psi_{1,2}$ creates a state that would correspond classically to two copies of global AdS_2 glued together, as predicted by the "naive" classical limit of the differential equation discussed in the previous section. The $\psi_{1,3}$ contribution is sensitive to the boundary conditions, and will be analyzed in the next subsection for a specific choice of boundary type.

2.4.2 $(1,1;1,2)$ boundary condition

Let us now specialize to the strip with $(1,1)$ boundary condition on the left and $(1,2)$ boundary condition on the right. The only allowed boundary primary operator/state is $\psi_{1,2}$. To compute the expectation value of the Liouville field in this state, we need to compute the bulk-boundary three point function $\langle\psi_{1,2}(y_1)\psi_{1,2}(y_2)V_\alpha(z)\rangle$, with $(1,1)$ boundary condition on one segment of the boundary circle and $(1,2)$ boundary on the other segment of the circle, between y_1 and y_2, as shown in figure 2. There are two different ways to factorize $\langle\psi_{1,2}(y_1)\psi_{1,2}(y_2)V_\alpha(z)\rangle$ into the product of a boundary three point function and a bulk-boundary two point function, along channels of $(1,1;1,1)$ boundary type or $(1,2;1,2)$ boundary type. In the first factorization, as shown in figure 3, the only boundary primary operator in the channel is the identity operator. We have then

$$\langle\psi(y_1)\psi(y_2)V_\alpha(z)\rangle = |z-\bar{z}|^{-2\Delta_\alpha}(y_1-y_2)^{-2h}U_{1,1}(\alpha)(1-\eta)^{\alpha/b}{}_2F_1\left(\frac{2\alpha}{b},1+b^{-2};2+2b^{-2};\eta\right)\,. \tag{2.36}$$

In the second factorization, we have the identity operator as well as $\psi_{1,3}$ propagating

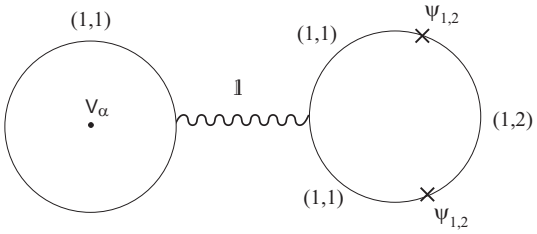

Figure 3. Factorization of the bulk-boundary three point function along the $(1,1;1,1)$ channel.

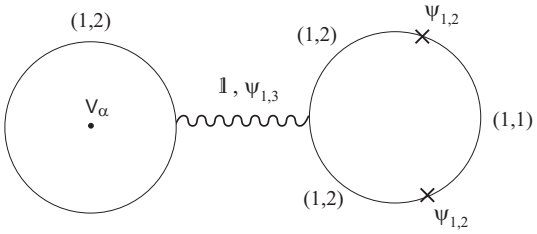

Figure 4. Factorization of the bulk-boundary three point function along the $(1,2;1,2)$ channel.

through the channel, as depicted in figure 3, giving

$$\begin{aligned}\langle\psi(y_1)\psi(y_2)V_\alpha(z)\rangle \;=\; &|z-\bar{z}|^{-2\Delta_\alpha}(y_1-y_2)^{-2h}\Big[U_{1,2}(\alpha)(1-\bar{\eta})^{\alpha/b}{}_2F_1\left(\frac{2\alpha}{b},1+b^{-2};2+2b^{-2};\bar{\eta}\right)\\ &-ie^{-i\pi/b^2}\langle\psi_{1,2}\psi_{1,2}\psi_{1,3}\rangle R_{1,3}(\alpha)(1-\bar{\eta})^{\alpha/b}\bar{\eta}^{-1-2b^{-2}}\\ &\times{}_2F_1\left(-1-2b^{-2}+\frac{2\alpha}{b},-b^{-2};-2b^{-2};\bar{\eta}\right)\Big],\end{aligned}\tag{2.37}$$

where $\bar{\eta}$ is the complex conjugate of η. One may also replace $\bar{\eta}$ by $\eta/(\eta-1)$, and use the property of Gauss hypergeometric functions to rewrite (2.37) in terms of the same functions with argument η. The phase factor $-ie^{-i\pi/b^2}$ in the second term on the r.h.s. is such that in the factorization limit $\eta\to i\epsilon$ ($\sigma\to\pi-\epsilon$), the conformal block corresponding to the $\psi_{1,3}$ is real and positive. One may seem to run into a puzzle here, since the two ways of factorizing the bulk-boundary three point function should give the same result. The resolution is that in fact (2.36) and (2.37) are related by analytic continuation across the branch cut of the hypergeometric function from $\eta=1$ to infinity. This can be shown using the monodromy of the hypergeometric function around $\eta=1$, or equivalently

$$\begin{aligned}{}_2F_1(a,b;c;x+i\epsilon) \;=\; &e^{2\pi i(a+b-c)}{}_2F_1(a,b;c;x)\\ &+2\pi i e^{\pi i(a+b-c)}\frac{\Gamma(c)}{\Gamma(a+b+1-c)\Gamma(c-a)\Gamma(c-b)}\,{}_2F_1(a,b;a+b+1-c;1-x)\end{aligned}\tag{2.38}$$

for real $x>1$, together with the boundary three point function $\langle\psi_{1,2}\psi_{1,2}\psi_{1,3}\rangle$ which will be explicitly computed below.

To compute $\langle\psi_{1,2}\psi_{1,2}\psi_{1,3}\rangle$, we make use of the boundary four point function $\langle\psi_{1,2}(y_1)\psi_{1,2}(y_2)\psi_{1,2}(y_3)\psi_{1,2}(y_4)\rangle$, with alternating $(1,1)$ and $(1,2)$ boundary conditions

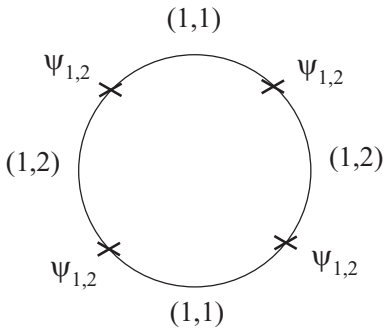

Figure 5. Boundary four point function with alternating boundary conditions.

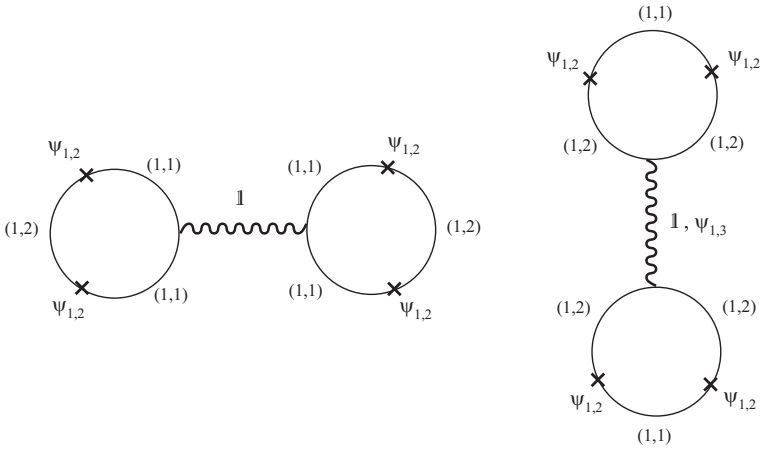

Figure 6. The two possible factorizations of the boundary four point function.

along the four segments of the boundary circle separated by the boundary operators, see figure 5. It is determined by a function $\mathcal{G}(\zeta)$,

$$\begin{aligned}\langle\psi_{1,2}(y_1)\psi_{1,2}(y_2)\psi_{1,2}(y_3)\psi_{1,2}(y_4)\rangle &= (y_1-y_2)^{-2h_{1,2}}(y_3-y_4)^{-2h_{1,2}}\mathcal{G}(\zeta),\\ \zeta &= \frac{(y_1-y_2)(y_3-y_4)}{(y_3-y_2)(y_1-y_4)}\,.\end{aligned} \tag{2.39}$$

$\mathcal{G}(\zeta)$ satisfies the same differential equation as that of $\mathcal{F}(\eta)$, with Δ_α replaced by h ($\alpha \to -\frac{1}{2b}$), η replaced by ζ. The solutions takes the form

$$\begin{aligned}\mathcal{G}(\zeta) = {}& c_1(1-\zeta)^{-\frac{1}{2}b^{-2}}{}_2F_1(-b^{-2},1+b^{-2};2+2b^{-2};\zeta)\\ &+c_2(1-\zeta)^{-\frac{1}{2}b^{-2}}\zeta^{-1-2b^{-2}}{}_2F_1(-1-3b^{-2},-b^{-2};-2b^{-2};\zeta)\,.\end{aligned} \tag{2.40}$$

Again, we can factorize it into two boundary three point functions, along either $(1,1;1,1)$ channel (with the only primary being the identity operator) or $(1,2;1,2)$ channel (with primaries $\mathbf{1}$ and $\psi_{1,3}$). The two factorizations are shown in figure 6. The first factoriza-

JHEP07(2009)002

tion gives

$$\langle\psi_{1,2}(y_1)\psi_{1,2}(y_2)\psi_{1,2}(y_3)\psi_{1,2}(y_4)\rangle = (y_1-y_2)^{-2h_{1,2}}(y_3-y_4)^{-2h_{1,2}} \times(1-\zeta)^{-\frac{1}{2}b^{-2}}{}_2F_1(-b^{-2},1+b^{-2};2+2b^{-2};\zeta)\,, \tag{2.41}$$

while the second factorization gives

$$\begin{aligned}\langle\psi_{1,2}(y_1)\psi_{1,2}(y_2)\psi_{1,2}(y_3)\psi_{1,2}(y_4)\rangle =& \\ C(b)(y_1-y_2)^{-2h_{1,2}}(y_3-y_4)^{-2h_{1,2}}&\left(\frac{1-\zeta}{\zeta}\right)^{-2h_{1,2}} \\ \times\Big[\zeta^{-\frac{1}{2}b^{-2}}&{}_2F_1(-b^{-2},1+b^{-2};2+2b^{-2};1-\zeta) \\ +\langle\psi_{1,2}\psi_{1,2}\psi_{1,3}\rangle^2\,\zeta^{-\frac{1}{2}b^{-2}}&(1-\zeta)^{-1-2b^{-2}}{}_2F_1(-1-3b^{-2},-b^{-2};-2b^{-2};1-\zeta)\Big]\end{aligned} \tag{2.42}$$

where $C(b) = -(2\cos(\pi b^{-2}))^{-1}$ is a normalization factor (which can be determined by matching the two channels as explained below). This nontrivial normalization factor is due to the different boundary conditions on the channels of the two factorizations. In fact, we can identify

$$C(b) = \frac{C_{1,1}(b)}{C_{1,2}(b)} \tag{2.43}$$

where $C_{m,n}(b)$ stands for the disc amplitude with no insertions and (m,n) boundary condition. The forms of (2.41) and (2.42) agree by the identity

$$\begin{aligned}{}_2F_1(A,B;C;z) =& \frac{\Gamma(C)\Gamma(C-A-B)}{\Gamma(C-A)\Gamma(C-B)}{}_2F_1(A,B;A+B+1-C;1-z) \\ &+\frac{\Gamma(C)\Gamma(A+B-C)}{\Gamma(A)\Gamma(B)}(1-z)^{C-A-B}{}_2F_1(C-A,C-B;1+C-A-B;1-z) \\ =& (1-z)^{C-A-B}{}_2F_1(C-A,C-B;C;z).\end{aligned} \tag{2.44}$$

Using this, we then derive the boundary three point function

$$\langle\psi_{1,2}\psi_{1,2}\psi_{1,3}\rangle = \pm\left[-2\cos(\frac{\pi}{b^2})\frac{\Gamma(1+\frac{2}{b^2})\Gamma(2+\frac{2}{b^2})}{\Gamma(1+\frac{1}{b^2})\Gamma(2+\frac{3}{b^2})}\right]^{\frac{1}{2}}. \tag{2.45}$$

In order to match (2.36) and (2.37) through analytic continuation, as explained above, we need to choose the negative sign in (2.45). Using the results of [8], it follows that

$$\frac{\langle\psi_{1,2}\psi_{1,2}\psi_{1,3}\rangle R_{1,3}(\alpha)}{U_{1,1}(\alpha)} = -\frac{8}{\pi}\left(1+\frac{2}{b^2}\right)\sin\left(2\pi\frac{\alpha}{b}\right)\sin\left(2\pi\frac{\alpha-b^{-1}}{b}\right)\frac{\Gamma(\frac{2}{b^2})^2\Gamma(1-\frac{2\alpha}{b})\Gamma(-1-\frac{2}{b^2}+\frac{2\alpha}{b})}{\Gamma\left(\frac{1}{b^2}\right)^2}. \tag{2.46}$$

It is also useful to note the identity

$$\frac{U_{1,2}(\alpha)}{U_{1,1}(\alpha)} = \frac{\cos(\pi(\frac{2\alpha}{b}-\frac{1}{b^2}))}{\cos(\pi/b^2)}. \tag{2.47}$$

Using (2.46) and (2.47), remarkably, one can check that (2.37) is indeed related to (2.36) by analytic continuation to a different sheet across its branch cut. This also provides a check of the result of [8] for $U_{m,n}(\alpha)$ and $R_{1,3}(\alpha)$.

JHEP07(2009)002

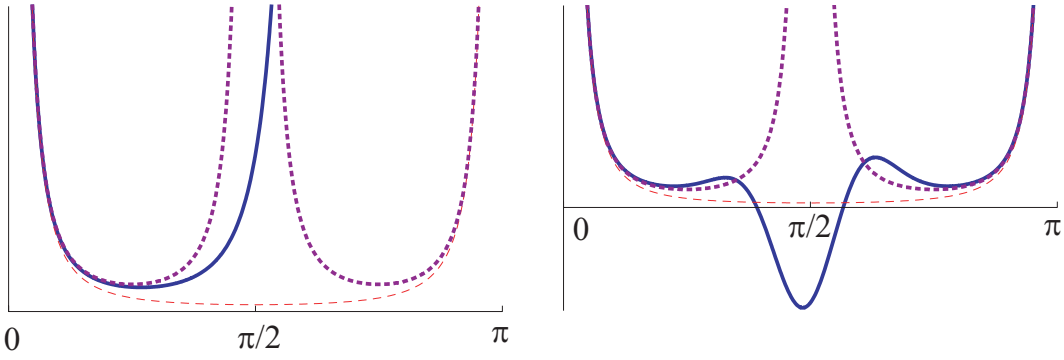

Figure 7. Plots of the bulk-boundary 3-point function $\langle\psi_{1,2}|V_\alpha(\sigma)|\psi_{1,2}\rangle$ (with $\alpha = b$) at finite coupling, for b real (left) and b imaginary (right), with $|b| = 0.3$. The dashed line represents the AdS_2 metric, while the dotted one corresponds to the two-fragmented AdS_2. With real b (left) the asymptotic AdS_2 boundary condition is respected only at the $\sigma = 0$ boundary, and the classical limit $b \to 0$ produces a single AdS_2 fragment (the solid line extends to $\sigma = \pi$ and erases the second AdS_2). On the other hand, with imaginary b (right) the profile is asymptotically AdS_2 at both boundaries and the limit $b \to 0$ gives the two-fragmented AdS_2 metric.

The quantum bulk-boundary three-point function can therefore be determined by analytically continuing (2.36) from $\sigma = 0$ to $\sigma = \pi$. In practice, such analytic continuation may be defined by "patching" (2.36) to (2.37) at $\sigma = \pi/2$, while using the standard definition of the hypergeometric functions with their conventional branch cuts. On the two halves of the strip, we find in the $b \to 0$ limit, with α/b finite,

$$\begin{aligned}
&\langle\psi_{1,2}|e^{2\alpha\phi(\sigma)}|\psi_{1,2}\rangle \sim U_{1,1}(\alpha)(\sin 2\sigma)^{-2\alpha/b}, \qquad \sigma \in \left(0, \frac{\pi}{2}\right), \\
&\langle\psi_{1,2}|e^{2\alpha\phi(\sigma)}|\psi_{1,2}\rangle \sim U_{1,2}(\alpha)\,(\sin 2\sigma)^{-2\alpha/b} \\
&\qquad\qquad + \langle\psi_{1,2}\psi_{1,2}\psi_{1,3}\rangle R_{1,3}(\alpha)(2\sin\sigma)^{-1-2b^{-2}-2\alpha/b}(\cos\sigma)^{2\alpha/b-1}, \qquad \sigma \in \left(\frac{\pi}{2}, \pi\right).
\end{aligned} \tag{2.48}$$

We see that for real b and generic values of α, in the classical limit the $\psi_{1,3}$ channel dominates for $\sigma > \pi/2$, and appears to "erase" the right AdS_2. The exceptional cases are when the probe bulk operator has $\alpha = -nb/2$ for a positive integer n, and $R_{1,3}(\alpha)$ vanishes. In this case the hypergeometric function reduces to elementary functions. For instance, when $\alpha = -b/2$, we have

$$\langle\psi_{1,2}|e^{-b\phi(\sigma)}|\psi_{1,2}\rangle = \frac{\sin 2\sigma}{2}(\sin\sigma)^{\frac{3}{2}b^2} \tag{2.49}$$

agreeing with the "naive" classical limit of two-fragmented AdS_2.

On the other hand, we can consider $b = i\beta$ purely imaginary, and take α to be purely imaginary as well (or equivalently, Wick rotating the Liouville field ϕ). In the classical limit $\beta \to 0$ (α/b taken to be real and finite), the identity channel dominates the $\psi_{1,3}$ channel, and we have

$$\begin{aligned}
&\langle\psi_{1,2}|e^{2\alpha\phi(\sigma)}|\psi_{1,2}\rangle \sim U_{1,1}(\alpha)(\sin 2\sigma)^{-2\alpha/b}, \qquad \sigma \in \left(0, \frac{\pi}{2}\right), \\
&\langle\psi_{1,2}|e^{2\alpha\phi(\sigma)}|\psi_{1,2}\rangle \sim U_{1,2}(\alpha)(\sin 2\sigma)^{-2\alpha/b}, \qquad \sigma \in \left(\frac{\pi}{2}, \pi\right),
\end{aligned} \tag{2.50}$$

JHEP07(2009)002

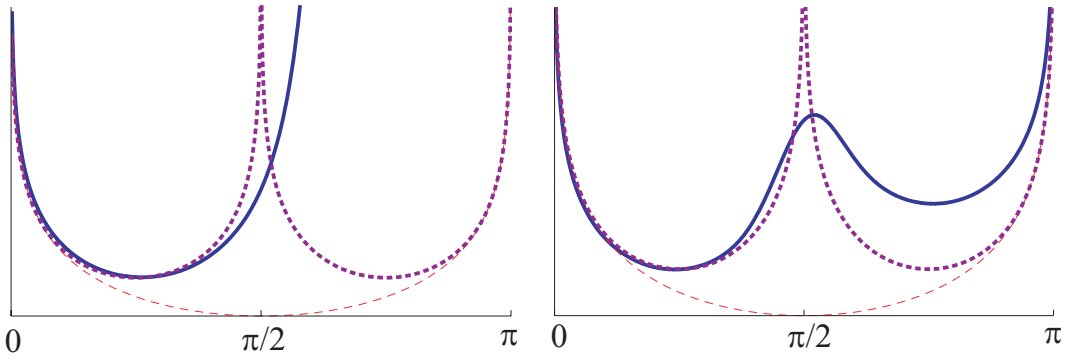

Figure 8. Plots of the expectation value of $\phi(\sigma)$ in the ZZ boundary primary $|\psi_{1,2}\rangle$, for b real (left) and b imaginary (right), with a generic non-integer value of $|b^{-2}|$. The dashed line represents the Liouville profile of the AdS_2 vacuum, while the dotted one corresponds to the two-fragmented AdS_2. In the case of imaginary b, the profile of the Liouville field on the right AdS_2 is shifted by the constant $\frac{2\pi}{b}\tan(\pi/b^2)$.

i.e. the expectation value of $e^{2\alpha\phi(\sigma)}$ scales like $(\sin 2\sigma)^{-2\alpha/b}$ on both halves of the strip, leading to two-fragmented AdS_2. Plots of the analytically continued bulk-boundary three point function for real and purely imaginary b are given in figure 7.

We see that near the mid point $\sigma = \pi/2$ where the two fragmented AdS_2's meet, quantum correction is large despite that the conformal dimension of the probe operator $\Delta_\alpha \sim \alpha/b \ll |c|$. In particular, the expectation value of $V_\alpha(\sigma = \pi/2)$ in the state $|\psi_{1,2}\rangle$ is given by (using the quadratic transform of ${}_2F_1$)

$$\begin{aligned}\langle\psi_{1,2}|e^{2\alpha\phi(\pi/2)}|\psi_{1,2}\rangle &= {}_2F_1\left(\frac{\alpha}{b}, 1+b^{-2}-\frac{\alpha}{b}; \frac{3}{2}+b^{-2}; 1\right)\\ &= \frac{\sqrt{\pi}\,\Gamma(\frac{3}{2}+b^{-2})}{\Gamma(\frac{1}{2}+\frac{\alpha}{b})\Gamma(\frac{3}{2}+b^{-2}-\frac{\alpha}{b})}\\ &\to \begin{cases} b^{-2\alpha/b}\frac{\sqrt{\pi}}{\Gamma(\frac{1}{2}+\frac{\alpha}{b})}, & b\to+0,\\ (-b^2)^{-\alpha/b}\frac{\cos(\pi(\frac{\alpha}{b}-b^{-2}))}{\cos(\pi b^{-2})}\frac{\sqrt{\pi}}{\Gamma(\frac{1}{2}+\frac{\alpha}{b})}, & b\to i0.\end{cases}\end{aligned} \tag{2.51}$$

For instance, for imaginary b, $\langle\psi_{1,2}|e^{2b\phi(\sigma)}|\psi_{1,2}\rangle$ is negative at $\sigma = \pi/2$, as in figure 7.

It is natural to consider V_α in the $\Delta_\alpha \sim \alpha/b \to 0$ limit. We find for b purely imaginary, in the $b \to i0$ limit,

$$\begin{aligned}\langle\psi_{1,2}|\phi(\sigma)|\psi_{1,2}\rangle &= \frac{1}{2}\frac{\partial}{\partial\alpha}\langle\psi_{1,2}|V_\alpha(\sigma)|\psi_{1,2}\rangle\Big|_{\alpha=0}\\ &\to \begin{cases} -\frac{1}{b}\ln|\sin 2\sigma| + const, & \sigma\in(0,\frac{\pi}{2}),\\ -\frac{1}{b}\ln|\sin 2\sigma| + \frac{2\pi}{b}\tan(\pi/b^2) + const, & \sigma\in(\frac{\pi}{2},\pi),\end{cases}\end{aligned} \tag{2.52}$$

where the overall constant shift can be absorbed into the Liouville cosmological constant. Curiously, the profile of the Liouville field in the two AdS_2's differ by a constant shift $\frac{2\pi}{b}\tan(\pi/b^2)$, coming from the derivative of $U_{1,2}(\alpha)/U_{1,1}(\alpha)$ at $\alpha = 0$, which is oscillatory

JHEP07(2009)002

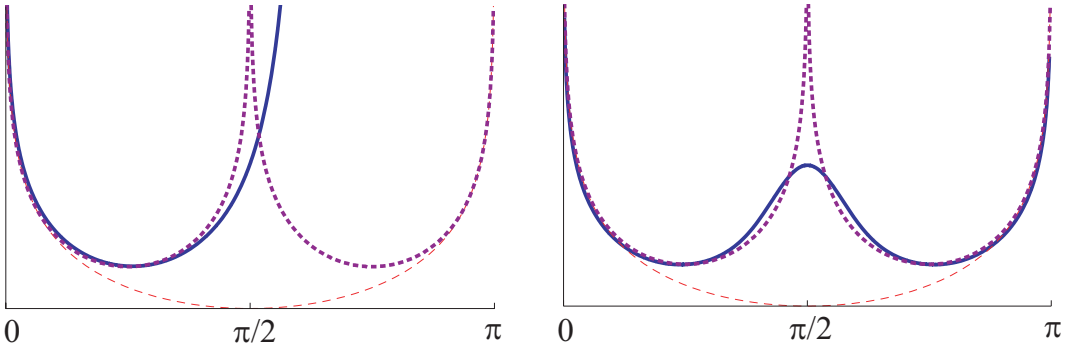

Figure 9. Plots of the expectation value of $\phi(\sigma)$ in the ZZ boundary primary $|\psi_{1,2}\rangle$, for b real (left) and b imaginary (right), with the integer value of $|b^{-2}| = 16$. The dashed line represents the Liouville profile of the AdS_2 vacuum, while the dotted one corresponds to the two-fragmented AdS_2.

as $b \to 0$. At the special values $b = i/\sqrt{n}$, for positive integer n, this shift is absent and we have a regular semi-classical limit as $n \to \infty$. This suggests a quantization of the central charge in Liouville AdS_2 gravity, $c = 1 + 6Q^2 = 13 - 6(n + \frac{1}{n})$.

To summarize the results of this section, we found that:

1. For real values of b, in the $b \to 0$ limit, only one of the two AdS_2 fragments survives in the quantum theory, and the geometry of the ZZ boundary primary $\psi_{1,2}$ is asymptotically AdS_2 only near the $(1,1)$ boundary, while destroying the AdS_2 boundary condition on the $(1,2)$ boundary. However, the bulk operators $V_{-nb/2}$ for positive integer n still see the two-fragmented AdS_2.

2. For purely imaginary values of b, the ZZ boundary primary $\psi_{1,2}$ creates two-fragmented AdS_2 in the semi-classical limit, which survives in the quantum theory. A regular semi-classical limit also suggests the quantization of the Liouville central charge, $b = i/\sqrt{n}$ and $c = 1 + 6Q^2 = 13 - 6(n + \frac{1}{n})$, where n is a positive integer.

Perhaps it is worth recalling here that purely imaginary b is the required choice if one wishes to consistently couple the Liouville sector to a unitary matter CFT, in the semi-classical limit.

2.5 Probing $|\psi_{m,n}\rangle$ with degenerate bulk primaries

In this subsection, we consider the bulk-boundary three point function involving the first degenerate bulk primary $V_{-b/2}$ and general ZZ boundary primary $\psi_{m,n}$ with $(1,1)$ boundary condition on one side of the disc and (m,n) boundary condition on the other side,

$$\langle \psi_{m,n}(y_1)\psi_{m,n}(y_2)V_{-b/2}(z,\bar{z})\rangle = |z-\bar{z}|^{1+\frac{3}{2}b^2} y_{12}^{-2h_{m,n}} \mathcal{F}(\eta)\,. \tag{2.53}$$

The null state at level 2 in the conformal family of $V_{-b/2}$ gives rise to a second order differential equation on $\mathcal{F}(\eta)$. The two independent solutions to the differential equation are conformal blocks corresponding to the factorization on the identity operator and $\psi_{1,3}$.

Since we have chosen the $(1,1)$ boundary condition at $\sigma = 0$, then the factorization through $\psi_{1,3}$ channel is absent as $V_{-b/2}$ approaches the left boundary. This fixes the solution to

$$\mathcal{F}(\eta) = (1-\eta)^{\frac{n+1+(m+1)b^2}{2}} {}_2F_1(n+1+(m+1)b^2, 1+b^2; 2+2b^2; \eta) \tag{2.54}$$

or in terms of the expectation value of $V_{-b/2}$ on the strip,

$$\begin{aligned}\langle \psi_{m,n}|e^{-b\phi(\sigma)}|\psi_{m,n}\rangle &= (\sin\sigma)^{1+\frac{3}{2}b^2} e^{i(n+1+(m+1)b^2)\sigma} {}_2F_1(n+1+(m+1)b^2, 1+b^2; 2+2b^2; 1-e^{2i\sigma}) \\ &\to \frac{\sin(n\sigma)}{n} \qquad (b\to 0)\,,\end{aligned} \tag{2.55}$$

confirming the interpretation of $\psi_{m,n}$ as n-fragmented AdS_2 in the semi-classical limit. Although, we should note that we expect the same subtlety in the case of real b discussed in the previous section, where generic V_α will only see one of the n AdS_2's, the other fragments being "erased" by quantum effects. For purely imaginary b, however, we expect the n-fragmented AdS_2 to survive in the full quantum theory.

3 Interactions of fragmented AdS_2

3.1 Boundary three-point functions

Let us denote by $\langle m,n,k\rangle$ the boundary three-point function $\langle \psi_{1,m}\psi_{1,n}\psi_{1,k}\rangle$ with boundary condition of $(1,2)$ type between $\psi_{1,m}$ and $\psi_{1,n}$ insertions, $(1,n-1)$ between $\psi_{1,n}$ and $\psi_{1,k}$, and $(1,m-1)$ between $\psi_{1,m}$ and $\psi_{1,k}$. Note that $\langle m,n,k\rangle$ is not symmetric in n,k,m. In the classical limit, however, we have seen that the profile of $\psi_{1,m}$ is not sensitive to the boundary types, provided that the primary $\psi_{1,m}$ is contained in the Hilbert space of the given boundary types. So we expect that the classical limit of $\langle m,n,k\rangle$ to be symmetric in m,n,k. We will find that this is indeed the case, apart from an oscillating factor. Also note that $\langle m,n,k\rangle$ is nonzero only when $|m-n|+1 \le k \le m+n-3$ and $m+n+k+1 \in 2\mathbb{Z}$, due to the selection rule (2.4).

We shall consider the boundary four-point function $\langle 2,m,k,n\rangle$, with boundary condition $(1,1;1,m;1,n-1;1,2)$ around the boundary circle. It can factorize as

$$\langle \psi_{1,2}\psi_{1,m}\psi_{1,k}\psi_{1,n}\rangle \to \langle \psi_{1,2}\psi_{1,n}\psi_{1,n-1}\rangle\langle \psi_{1,n-1}\psi_{1,2}\psi_{1,m}\rangle \tag{3.1}$$

or as (schematically)

$$\begin{aligned}\langle \psi_{1,2}\psi_{1,m}\psi_{1,k}\psi_{1,n}\rangle \to\ & \langle \psi_{1,2}\psi_{1,m}\psi_{1,m-1}\rangle\langle \psi_{1,m-1}\psi_{1,n}\psi_{1,k}\rangle \\ & + \langle \psi_{1,2}\psi_{1,m}\psi_{1,m+1}\rangle\langle \psi_{1,m+1}\psi_{1,n}\psi_{1,k}\rangle\,.\end{aligned} \tag{3.2}$$

Writing

$$\langle \psi_{1,2}(y_1)\psi_{1,m}(y_2)\psi_{1,k}(y_4)\psi_{1,n}(y_3)\rangle = (y_{12}y_{34})^{\sum h_i}\left(\prod_{1\le i<j\le 4} y_{ij}^{-h_i-h_j}\right)\mathcal{F}(\eta), \tag{3.3}$$

where $\eta = y_{12}y_{34}/y_{14}y_{32}$, $\mathcal{F}(\eta)$ obeys the hypergeometric equation coming from the null state in the conformal family of $\psi_{1,2}$. The general solution is

$$\mathcal{F}(\eta) = (1-\eta)^{(1-\frac{n}{2})(1+\frac{n}{2b^2})}\eta^{-1+\frac{n+k}{2}+\frac{n^2+k^2-2m}{4b^2}}\left[C_1\ {}_2F_1\left(\frac{n-m-k}{2b^2}, 1+\frac{n+k-m}{2b^2}; -\frac{m}{b^2}; \eta\right)\right.$$
$$\left. + C_2\eta^{1+\frac{m}{b^2}}\ {}_2F_1\left(1+\frac{n+m-k}{2b^2}, 2+\frac{n+m+k}{2b^2}; 2+\frac{m}{b^2}; \eta\right)\right]. \tag{3.4}$$

The limit $\eta \to 0$ corresponds to the factorization through $\psi_{m\pm1}$, whereas $\eta \to 1$ corresponds to the factorization though ψ_{n-1}. Imposing that there is no factorization through ψ_{n+1} (as required by our choice of boundary condition), we find

$$\frac{\langle m+1,2,m\rangle\langle m+1,n,k\rangle}{\langle m-1,2,m\rangle\langle m-1,n,k\rangle} = \frac{C_1}{C_2} = \frac{\Gamma(2+\frac{m}{b^2})\Gamma(\frac{k-m-n}{2b^2})\Gamma(-1-\frac{k+m+n}{2b^2})}{\Gamma(-\frac{m}{b^2})\Gamma(1+\frac{k+m-n}{2b^2})\Gamma(\frac{m-n-k}{2b^2})}$$
$$= \frac{\cos((n+k-3m)\frac{\pi}{2b^2}) - \cos((n+k+m)\frac{\pi}{2b^2})}{\cos(\frac{k\pi}{b^2}) - \cos(\frac{(m+n)\pi}{b^2})}\frac{\Gamma(1+\frac{m}{b^2})\Gamma(2+\frac{m}{b^2})\Gamma(1+\frac{n+k-m}{2b^2})}{\Gamma(1+\frac{k+m-n}{2b^2})\Gamma(1+\frac{m+n-k}{2b^2})\Gamma(2+\frac{k+m+n}{2b^2})}. \tag{3.5}$$

Choosing $n=2, k=m$, we obtain $\langle m+1,2,m\rangle/\langle m-1,2,m\rangle$; then we can further derive $\langle m+1,n,k\rangle/\langle m-1,n,k\rangle$. We shall not write the general formula, but focus on the classical limit $(b\to 0)$,

$$\frac{\langle m+1,n,k\rangle}{\langle m-1,n,k\rangle} \sim (oscillating\ factor)\times\exp\left[\frac{1}{b^2}(m\log(4m)+\frac{1}{2}(m-1)\log(m-1)\right.$$
$$+\frac{1}{2}(m+1)\log(m+1) - \frac{1}{2}(m+k-n)\log(m+k-n) - \frac{1}{2}(m-k+n)\log(m-k+n)$$
$$\left.+\frac{1}{2}(-m+k+n)\log(-m+k+n) - \frac{1}{2}(m+k+n)\log(m+k+n)) + \mathcal{O}(1)\right]. \tag{3.6}$$

Iterating this relation, we find

$$\frac{\langle 1+x,1+y,1+z\rangle}{\langle -1+x,-1+y,-1+z\rangle} \sim (oscillating\ factor)\times\exp\left[\frac{1}{b^2}(x\log(4x)+\frac{1}{2}(x-1)\log(x-1)\right.$$
$$+\frac{1}{2}(x+1)\log(x+1) + y\log(4y) + \frac{1}{2}(y-1)\log(y-1) + \frac{1}{2}(y+1)\log(y+1)$$
$$+z\log(4z) + \frac{1}{2}(z-1)\log(z-1) + \frac{1}{2}(z+1)\log(z+1)$$
$$-\frac{1}{2}(x+y-z)\log(x+y-z) - \frac{1}{2}(x-y+z)\log(x-y+z)$$
$$-\frac{1}{2}(-x+y+z)\log(-x+y+z) - \frac{1}{2}(x+y+z)\log(x+y+z)$$
$$\left.-\frac{1}{2}(x+y+z-2)\log(x+y+z-2) - \frac{1}{2}(x+y+z+2)\log(x+y+z+2)) + \mathcal{O}(1)\right]. \tag{3.7}$$

This expression is particularly interesting because, as we will show in section 3.4 below, an analytic continuation to non-integer x, y, z can be matched against the geodesic approximation of three point particles in AdS_2.

JHEP07(2009)002

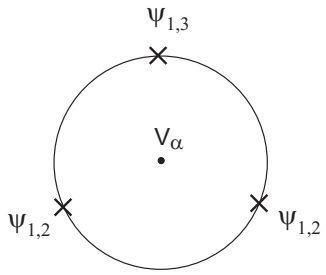

Figure 10. The bulk-boundary four point function.

We can also give a closed form expression in the limit $x, y, z \gg 1$, corresponding to the scattering of AdS_2's with many fragments. In this case, we get

$$\langle x, y, z\rangle \sim \exp\left[\frac{1}{b^2}(x^2\log x + y^2\log y + z^2\log z - \frac{(x+y-z)^2}{4}\log(x+y-z)\right.$$
$$\left. -\frac{(x-y+z)^2}{4}\log(x-y+z) - \frac{(-x+y+z)^2}{4}\log(-x+y+z) - \frac{(x+y+z)^2}{4}\log(x+y+z))\right]. \tag{3.8}$$

3.2 Bulk-boundary four-point functions

In this section we study the disc bulk-boundary four-point function $\langle\psi_{1,2}(y_1)\psi_{1,2}(y_2)\psi_{1,3}(y_3)V_\alpha(z,\bar{z})\rangle$, see figure 10. The choice of boundary type is not important for now, since we will be interested in the classical limit of this correlation function. By conformal invariance, this four-point function takes the form

$$\langle\psi_{1,2}(y_1)\psi_{1,2}(y_2)\psi_{1,3}(y_3)V_\alpha(z,\bar{z})\rangle = |z-\bar{z}|^{-2\Delta_\alpha} y_{12}^{-2h_{1,2}+h_{1,3}}(y_{13}y_{23})^{-h_{1,3}}\mathcal{F}(\eta,\bar{\eta}) \tag{3.9}$$

where

$$\eta = \frac{(z-y_1)y_{23}}{(z-y_3)y_{21}}, \qquad \bar{\eta} = \frac{(\bar{z}-y_1)y_{23}}{(\bar{z}-y_3)y_{21}}. \tag{3.10}$$

We can use the $\mathrm{SL}(2,\mathbb{R})$ symmetry to fix for example $y_1 = 0, y_2 = 1$ and $y_3 = \infty$. Then η and $\bar{\eta}$ simply coincide with the coordinates z and $\bar{z}$ parameterizing the position of the "probe" bulk primary $V_\alpha(z,\bar{z})$.

The constraining equation from the level 2 null state in the conformal family of $\psi_{1,2}(y_1)$ reduces to a second order differential equation on $\mathcal{F}$,

$$\Delta_\alpha(\eta-\bar{\eta})^2\mathcal{F} + \bar{\eta}^2\eta(\eta-1)(2(1+b^2)\eta+1)\partial_\eta\mathcal{F} + \eta^2\bar{\eta}(\bar{\eta}-1)(2(1+b^2)\bar{\eta}+1)\partial_{\bar{\eta}}\mathcal{F} \tag{3.11}$$
$$+b^2\eta^2\bar{\eta}^2\left[(\eta-1)^2\partial_\eta^2\mathcal{F} + (\bar{\eta}-1)^2\partial_{\bar{\eta}}^2\mathcal{F} + 2|\eta-1|^2\partial_\eta\partial_{\bar{\eta}}\mathcal{F}\right] = 0\,.$$

In the classical limit $b \to 0$ (with $\frac{\alpha}{b}$ fixed), this reduces to the first order equation

$$\Delta_\alpha(\eta-\bar{\eta})^2\mathcal{F}^{cl} + \bar{\eta}^2\eta(\eta-1)(2\eta+1)\partial_\eta\mathcal{F}^{cl} + \eta^2\bar{\eta}(\bar{\eta}-1)(2\bar{\eta}+1)\partial_{\bar{\eta}}\mathcal{F}^{cl} = 0\,. \tag{3.12}$$

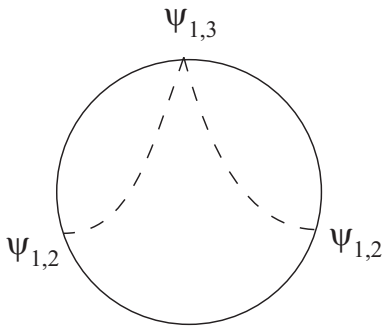

Figure 11. Schematic depiction of the classical solution (3.15), corresponding to three Poincaré discs patched together along the dashed lines.

Similarly, there is another equation coming from $\psi_{1,2}(y_2)$, which is identical to the above equation with $\mathcal{F}(\eta,\bar\eta)$ replaced by $\mathcal{F}(1-\eta,1-\bar\eta)$. The solution to this pair of equations is (up to a normalization constant)

$$\mathcal{F}^{cl}(\eta,\bar\eta) = \left[|\eta|^2|1-\eta|^2(2\eta^2+2\bar\eta^2+2|\eta|^2-3\eta-3\bar\eta)^{-2}\right]^{\Delta_\alpha}. \tag{3.13}$$

This means that if the classical limit of the three-point function $\langle\psi_{1,2}(y_1)\psi_{1,2}(y_2)\psi_{1,3}(y_3)\rangle$ is dominated by an instanton solution, the solution has Liouville profile

$$\langle e^{2\alpha\phi}\rangle_{\rm inst} = |z-\bar z|^{-2\alpha/b}\left[|z|^2|1-z|^2(2z^2+2\bar z^2+2|z|^2-3z-3\bar z)^{-2}\right]^{\alpha/b}. \tag{3.14}$$

The instanton solution has "physical" metric (we fix the overall normalization to agree with the conventions of ZZ)

$$e^{2b\phi}dzd\bar z = \frac{36|z|^2|1-z|^2dzd\bar z}{\pi b^2|z-\bar z|^2(2z^2+2\bar z^2+2|z|^2-3z-3\bar z)^2}. \tag{3.15}$$

This is indeed a solution to Liouville equation, and corresponds to three Poincaré discs patched together, depicted schematically in figure 11. In the upper half plane coordinate $z=x+iy$, the three disconnected AdS_2's are glued along the two curves

$$y=\sqrt{3x(x-1)}, \qquad x<0 \text{ or } x>1. \tag{3.16}$$

A contour plot of the classical solution (3.15) in the upper half plane coordinates, showing the curves (3.16) is shown in figure 12. It is also interesting to visualize the solution in the strip coordinates defined by $z=e^{i\sigma+\tau}$. The corresponding plot is shown in figure 13.

It is actually not difficult to obtain the classical instanton profile for more general boundary three point functions. Consider for example the four point function $\langle\psi_{1,3}(y_1)\psi_{1,3}(y_2)\psi_{1,3}(y_3)V_\alpha(z,\bar z)\rangle$. Again, by conformal invariance we can write

$$\langle\psi_{1,3}(y_1)\psi_{1,3}(y_2)\psi_{1,3}(y_3)V_\alpha(z,\bar z)\rangle = |z-\bar z|^{-2\Delta_\alpha}(y_{12}y_{13}y_{23})^{-h_{1,3}}\mathcal{F}_{333}(\eta,\bar\eta) \tag{3.17}$$

where η and $\bar\eta$ are defined as above. The constraining equation from the null state in the conformal family of $\psi_{1,3}(y_1)$, see eq. (2.19), reduces in the classical limit to the first order

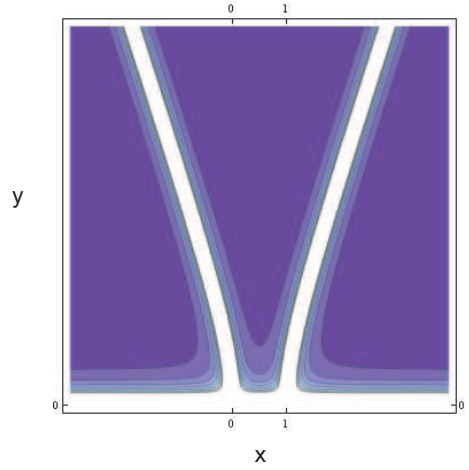

Figure 12. Contour plot of the solution (3.15) in the upper half plane coordinates. The points $x = 0$ and $x = 1$ on the real axis correspond to the insertions of the two $\psi_{1,2}$ operators. The "fragmentation lines" are described by eq. (3.16).

differential equation

$$2\Delta_\alpha(\eta-\bar\eta)^2(|\eta|^2-\eta-\bar\eta)\mathcal{F}^{cl}_{333}+\eta\bar\eta^3(\eta^2-1)(2\eta-1)\partial_\eta\mathcal{F}^{cl}_{333}+\bar\eta\eta^3(\bar\eta^2-1)(2\bar\eta-1)\partial_{\bar\eta}\mathcal{F}^{cl}_{333}=0\,, \tag{3.18}$$

and as before there is a similar equation coming from $\psi_{1,3}(y_2)$. The solution to this couple of first order differential equations (up to an overall constant) turns out to be

$$\mathcal{F}^{cl}_{333}(\eta,\bar\eta)=\left[\frac{|\eta|^2|1-\eta|^2}{(\eta^3+\bar\eta^3-2(\eta^2+\bar\eta^2)(|\eta|^2+1)+|\eta|^2(5\eta+5\bar\eta-2|\eta|^2-2))^2}\right]^{\Delta_\alpha}\,, \tag{3.19}$$

and the physical instanton metric ($\Delta_\alpha = 1$) corresponding to the three point function $\langle\psi_{1,3}\psi_{1,3}\psi_{1,3}\rangle$ is therefore

$$e^{2b\phi}dzd\bar z=\frac{36|z|^2|1-z|^2dzd\bar z}{\pi b^2|z-\bar z|^2\,(z^3+\bar z^3-2(z^2+\bar z^2)(|z|^2+1)+|z|^2(5z+5\bar z-2|z|^2-2))^2}. \tag{3.20}$$

One can verify that this is a solution to Liouville equation, and as expected corresponds to four copies of the Poincaré disc patched together.

3.3 Instantons interpolating fragmented AdS_2's

It is instructive to write the above solutions in the general form

$$e^{2b\phi}=\frac{1}{\pi b^2}\frac{\partial A(z)\bar\partial B(\bar z)}{(1-A(z)B(\bar z))^2}\,, \tag{3.21}$$

which is in fact the most general solution of Liouville equation

$$\partial\bar\partial\phi-\pi be^{2b\phi}=0\,. \tag{3.22}$$

JHEP07(2009)002

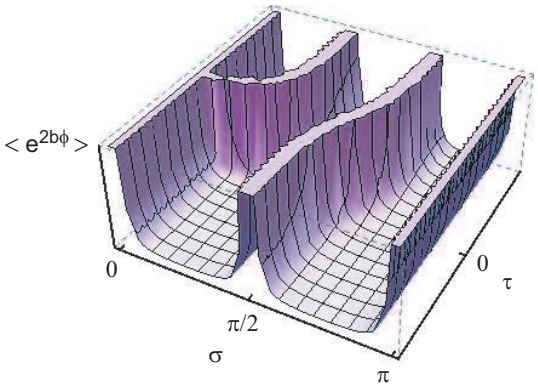

Figure 13. Strip coordinates plot of the classical Liouville profile corresponding to the boundary three point function $< \psi_{1,2}\psi_{1,2}\psi_{1,3} >$. The strip $\tau \in \mathbb{R}, 0 \leq \sigma \leq \pi$ fragments into three disconnected pieces.

For example, the regular AdS_2 solution corresponds to $B(\bar{z}) = 1/A(\bar{z})$ and $A(z) = z$, while the n-fragmented solution has $A(z) = z^n$. In fact, this is perhaps the fastest way to see that the stress tensor for the n-fragmented AdS_2 agrees with the conformal dimension of the operator $\psi_{1,n}$ (one simply looks at the Schwartzian derivative of the conformal transformation $w = z^n$).

Going back to the "instanton" solutions (3.15), (3.20) found above, one can see that they take indeed the form (3.21) (still with $B(\bar{z}) = 1/A(\bar{z})$, which ensures that the metric is real). By direct calculation one finds that $\partial A(z) = z(z-1)$ for the $\langle \psi_{1,2}\psi_{1,2}\psi_{1,3} \rangle$ and $\partial A(z) = \frac{z^2(z-1)^2}{(z-\frac{1}{2})^2}$ for the $\langle \psi_{1,3}\psi_{1,3}\psi_{1,3} \rangle$ case. Motivated by this, we conjecture that the general instanton solution corresponding to the three point function $\langle \psi_{1,n}(0)\psi_{1,m}(1)\psi_{1,k}(\infty) \rangle$ is given by[2]

$$\partial A(z) = \frac{z^{n-1}(z-1)^{m-1}}{P(z)^2}\,, \tag{3.23}$$

where $P(z)$ is a $(n+m-k-1)/2$-degree polynomial with distinct roots (to be determined below), namely $P(z) = \prod_{i=1}^{(n+m-k-1)/2}(z-z_i)$. Note that $(n+m-k-1)/2$ is an integer as implied by the three point function selection rules. The conjecture is motivated as follows. First, the degree of the zeroes at $z=0$ and $z=1$ and of the pole at $z=\infty$ are fixed by demanding that near those points the metric looks respectively like the n-fragmented, the m-fragmented and the k-fragemented AdS_2. Furthermore, the fact that $P(z)$ has distinct roots and the denominator of (3.23) is $P(z)^2$ follows by requiring that near each of the z_i the metric looks like the regular AdS_2. To see this, consider for simplicity $\partial A(z) \sim \frac{1}{(z-z_0)^s}$ near $z = z_0$. Then writing $z = z_0 + re^{i\theta}$, the metric close to z_0 takes the form

$$ds^2 \sim \frac{(dr/r)^2 + d\theta^2}{\sin^2((s-1)\theta)}\,,$$

[2]The metric (3.21) with $B = 1/\bar{A}$ is invariant under the $\mathrm{SL}(2,\mathbb{R})$ transformation $A \to (aA+b)/(cA+d)$, $\partial A \to \partial A/(cA+d)^2$. One can reach the standard form (3.23) by applying such $\mathrm{SL}(2,\mathbb{R})$ transformation.

JHEP07(2009)002

so that we have to choose $s = 2$ as claimed. Finally, whe have to specify the position of the roots z_i of $P(z)$. If we insist that $A(z)$ has to be a rational function, which seems to be a natural assumption, then the roots can be determined by requiring that the poles at $z = z_i$ have vanishing residue, namely

$$\frac{d}{dz}\left[(z-z_i)^2\partial A(z)\right]|_{z=z_i} = 0 \qquad i = 1, \cdots, \frac{n+m-k-1}{2}\,. \tag{3.24}$$

It is easy to verify that the above solutions for $\langle\psi_{1,2}\psi_{1,2}\psi_{1,3}\rangle$ and $\langle\psi_{1,3}\psi_{1,3}\psi_{1,3}\rangle$ satisfy the conjecture (3.23). By directly solving for the classical limit of the bulk-boundary four point function as described above, we have also successfully checked the conjecture on a few other explicit examples such as $\langle\psi_{1,2}\psi_{1,3}\psi_{1,4}\rangle$ and $\langle\psi_{1,3}\psi_{1,3}\psi_{1,5}\rangle$, which respectively have $\partial A(z) = z(z-1)^2$ and $\partial A(z) = z^2(z-1)^2$. Other tests of (3.23), (3.24) come from these known examples by applying an inversion $z \to 1/z$ to map the origin to infinity. For example, one finds that the solution for $\langle\psi_{1,3}(0)\psi_{1,2}(1)\psi_{1,2}(\infty)\rangle$ has $\partial A(z) = \frac{z^2(z-1)}{(z-2/3)^2}$ in agreement with the conjecture. A further check comes from $\langle\psi_{1,5}(0)\psi_{1,3}(1)\psi_{1,3}(\infty)\rangle$, which turns out to be given by $\partial A(z) = \frac{z^4(z-1)^2}{(z-z_1)^2(z-\bar{z}_1)^2}$ with $z_1 = \frac{1}{20}(15+i\sqrt{15})$, as predicted by (3.23), (3.24).

3.4 Comparison with the geodesic approximation

Consider the classical limit $b \to 0$ of the boundary three point function, for example eq. (2.45). In this limit one gets

$$\begin{aligned}
\langle\psi_{1,2}\psi_{1,2}\psi_{1,3}\rangle &\sim \pm\frac{2\sqrt{2}}{3^{\frac{3}{4}}}\left(-\cos\frac{\pi}{b^2}\right)^{\frac{1}{2}} e^{-\frac{1}{2b^2}\ln\frac{27}{16}}, && \text{real } b \to 0,\\
\langle\psi_{1,2}\psi_{1,2}\psi_{1,3}\rangle &\sim \pm\frac{\sqrt{2}}{3^{\frac{3}{4}}}\left(-\frac{1+2\cos\frac{2\pi}{b^2}}{\cos\frac{\pi}{b^2}}\right)^{\frac{1}{2}} e^{-\frac{1}{2b^2}\ln\frac{27}{16}}, && \text{imaginary } b \to 0.
\end{aligned} \tag{3.25}$$

The exponential term suggests that it should be possible to obtain this result by a semi-classical gravity calculation.[3] Namely one should evaluate the regularized action on the "instanton" solution, i.e. the classical Liouville profile (3.15), corresponding to the insertion of the three boundary primary operators, which was obtained in section 3.2. In this section we present a different calculation based on point particles moving along geodesics in AdS_2, which interestingly matches a particular analytic continuation of the boundary three point function discussed in section 3.1.

Consider three point particles of masses m_1, m_2, m_3 starting off at the boundary of the disk and moving along geodesics until they meet at one point in the interior. The geodesic approximation is expected to be valid when the mass of the particles are large compared to the AdS scale, and the gravity coupling is weak, i.e. in the limit $1 \ll m_i \ll 1/b^2$ (in AdS units). Mapping the problem to the upper half plane, we can place the particles with masses m_1 and m_2 on the real line (separated say by a distance L), and the particle with mass m_3 at $i\infty$. The particles m_1 and m_2 move along circles and m_3 along a straight line, until the geodesics meet at a certain height h, as shown in figure 14. Using as variables the final

[3] Curiously, for a special set of "quantized" values of b, namely $b^{-2} = n$ being an odd integer, the oscillatory factor on the r.h.s. of (3.25) is a constant independent n.

JHEP07(2009)002

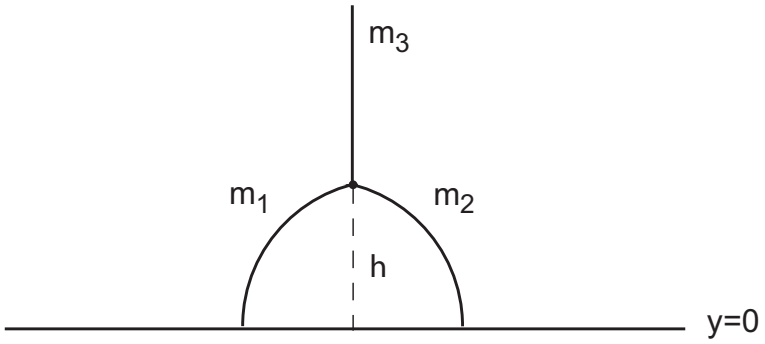

Figure 14. Three point particles of masses m_1, m_2, m_3 moving along geodesics in the Poincarè half plane.

angular position θ_1 and θ_2 of the circular geodesics, the total action for the system reads

$$S = m_1 \int_{\frac{\epsilon}{R_1}}^{\theta_1} \frac{d\theta}{\sin\theta} + m_2 \int_{\frac{\epsilon}{R_2}}^{\theta_2} \frac{d\theta}{\sin\theta} + m_3 \ln\frac{\Lambda}{h}\,, \tag{3.26}$$

where we have introduced cutoffs $\epsilon \to 0$ and $\Lambda \to \infty$. The geometry implies

$$h(\theta_1,\theta_2) = \frac{L}{\tan\frac{\theta_1}{2} + \tan\frac{\theta_2}{2}} \qquad\qquad R_{1,2} = \frac{h}{\sin\theta_{1,2}}\,. \tag{3.27}$$

Then one gets

$$\begin{aligned} S = {} & (m_1+m_2-m_3)\ln h - m_1 \ln\cos^2\frac{\theta_1}{2} - m_2 \ln\cos^2\frac{\theta_2}{2} \\ & -(m_1+m_2)\ln\epsilon + m_3 \ln\Lambda\,. \end{aligned} \tag{3.28}$$

It is not difficult to extremize this action with respect to θ_1 and θ_2 for general m_1, m_2, m_3. The solution turns out to be

$$\tan^2\frac{\theta_1}{2} = \frac{m_2^2-(m_1-m_3)^2}{(m_1+m_3)^2-m_2^2}\,, \qquad\qquad \tan^2\frac{\theta_2}{2} = \frac{m_1^2-(m_2-m_3)^2}{(m_2+m_3)^2-m_1^2}\,. \tag{3.29}$$

Plugging back into (3.28) and removing the divergencies, one finds the following general formula for the regularized action

$$\begin{aligned} S_{\rm reg} = \frac{1}{b^2}\Bigg[& \sum_{i=1}^{3} m_i \log(2m_i) - \frac{1}{2}(m_1+m_2-m_3)\log(m_1+m_2-m_3) \\ & -\frac{1}{2}(m_1-m_2+m_3)\log(m_1-m_2+m_3) - \frac{1}{2}(-m_1+m_2+m_3)\log(-m_1+m_2+m_3) \\ & -\frac{1}{2}(m_1+m_2+m_3)\log(m_1+m_2+m_3)\Bigg]\,. \end{aligned} \tag{3.30}$$

This expression matches the classical limit of the boundary three point function (3.7) if we take the masses to be $m_1 = -x/b^2, m_2 = -y/b^2, m_3 = -z/b^2$, with small real x, y, z. Note that the conformal dimension corresponding to a scalar of mass m is $h = \frac{1}{2} + \frac{1}{2}\sqrt{1+m^2}$ (where m is expressed in units of the AdS radius) [2]. In our limit $h \sim \frac{m}{2}$, consistently with the dimension $\Delta_{1,1+x} \sim -\frac{x}{2b^2}$ of the "analytically continued" operator $\psi_{1,1+x}$.

JHEP07(2009)002

Acknowledgments

We are grateful to D. Gaiotto, G. Moore, A. Pakman and D. Shih for useful discussions, and especially to A. Strominger for collaborations at the initial stage of this work and on related topics. X.Y. would like to thank Tata Insititute of Fundamental Research and the organizers of the Monsoon Workshop on String Theory for hospitality during the completion of this work. The work of S.G. is supported in part by the Center for the Fundamental Laws of Nature at Harvard University and by NSF grants PHY-024482 and DMS-0244464. The work of X.Y. is supported by a Junior Fellowship from the Harvard Society of Fellows.

References

[1] P.H. Ginsparg and G.W. Moore, *Lectures on $2-D$ gravity and $2-D$ string theory*, hep-th/9304011 [SPIRES].

[2] A. Strominger, *AdS_2 quantum gravity and string theory*, *JHEP* **01** (1999) 007 [hep-th/9809027] [SPIRES].

[3] J.M. Maldacena, J. Michelson and A. Strominger, *Anti-de Sitter fragmentation*, *JHEP* **02** (1999) 011 [hep-th/9812073] [SPIRES].

[4] A. Strominger, *A matrix model for AdS_2*, *JHEP* **03** (2004) 066 [hep-th/0312194] [SPIRES].

[5] T. Hartman and A. Strominger, *Central charge for AdS_2 quantum gravity*, *JHEP* **04** (2009) 026 [arXiv:0803.3621] [SPIRES].

[6] A. Sen, *Quantum entropy function from AdS_2/CFT_1 correspondence*, arXiv:0809.3304 [SPIRES].

[7] A. Sen, *Entropy function and AdS_2/CFT_1 correspondence*, *JHEP* **11** (2008) 075 [arXiv:0805.0095] [SPIRES].

[8] A.B. Zamolodchikov and A.B. Zamolodchikov, *Liouville field theory on a pseudosphere*, hep-th/0101152 [SPIRES].

[9] V. Fateev, A.B. Zamolodchikov and A.B. Zamolodchikov, *Boundary Liouville field theory. I: boundary state and boundary two-point function*, hep-th/0001012 [SPIRES].

[10] N. Seiberg, *Notes on quantum Liouville theory and quantum gravity*, *Prog. Theor. Phys. Suppl.* **102** (1990) 319 [SPIRES].

[11] Y. Nakayama, *Liouville field theory: a decade after the revolution*, *Int. J. Mod. Phys.* **A 19** (2004) 2771 [hep-th/0402009] [SPIRES].

[12] A.M. Polyakov, *Quantum geometry of bosonic strings*, *Phys. Lett.* **B 103** (1981) 207 [SPIRES].

[13] E. D'Hoker and R. Jackiw, *Liouville field theory*, *Phys. Rev.* **D 26** (1982) 3517 [SPIRES].

[14] E. D'Hoker, D.Z. Freedman and R. Jackiw, $SO(2,1)$ *invariant quantization of the Liouville theory*, *Phys. Rev.* **D 28** (1983) 2583 [SPIRES].

[15] N.M. Temme, *Large parameter cases of the Gauss hypergeometric function*, *J. Comput. Appl. Math.* **153** (2003) 441.

[16] P. Di Francesco, P. Mathieu and D. Senechal, *Conformal field theory*, Springer, New York U.S.A. (1997), pg. 890 [SPIRES].

JHEP07(2009)002